Earth and Planetary Science Letters 272 (2008) 330–338

Contents lists available at ScienceDirect

Earth and Planetary Science Letters

journal homepage: www.elsevier.com/locate/epsl

Nickel isotope heterogeneity in the early Solar System

Marcel Regelous [a,b,*], Tim Elliott [b], Christopher D. Coath [b]

[a] Department of Earth Sciences, Royal Holloway University of London, Egham, Surrey, TW20 0EX, UK
[b] Bristol Isotope Group, Department of Earth Sciences, Wills Memorial Building, Queen's Road, University of Bristol, BS8 1RJ, UK

ARTICLE INFO

Article history:
Received 24 December 2007
Received in revised form 25 April 2008
Accepted 1 May 2008
Available online 17 May 2008

Editor: R.W. Carlson

Keywords:
nickel isotopes
iron meteorites
chondrites
nucleosynthesis
short-lived nuclides
mass-independent fractionation

ABSTRACT

We report small but significant variations in the ^{58}Ni/^{61}Ni-normalised ^{60}Ni/^{61}Ni and ^{62}Ni/^{61}Ni ratios (expressed as ε^{60}Ni and ε^{62}Ni) of bulk iron and chondritic meteorites. Carbonaceous chondrites have variable, positive ε^{62}Ni (0.05 to 0.25), whereas ordinary chondrites have negative ε^{62}Ni (−0.04 to −0.09). The Ni isotope compositions of iron meteorites overlap with those of chondrites, and define an array with negative slope in the ε^{60}Ni versus ε^{62}Ni diagram. The Ni isotope compositions of the volatile-depleted Group IVB irons are similar to those of the refractory CO, CV carbonaceous chondrites, whereas the other common magmatic iron groups have Ni isotope compositions similar to ordinary chondrites. Only enstatite chondrites have identical Ni isotope compositions to Earth and so appear to represent the most appropriate terrestrial building material. Differences in ε^{62}Ni reflect distinct nucleosynthetic components in precursor solids that have been variably mixed, but some of the ε^{60}Ni variability could reflect a radiogenic component from the decay of ^{60}Fe. Comparison of the ε^{60}Ni of iron and chondritic meteorites with the same ε^{62}Ni allows us to place upper limits on the ^{60}Fe/^{56}Fe of planetesimals during core segregation. We estimate that carbonaceous chondrites had initial ^{60}Fe/^{56}Fe $<1\times10^{-7}$. Our data place less good constraints on initial ^{60}Fe/^{56}Fe ratios of ordinary chondrites but our results are not incompatible with values as high as 3×10^{-7} as determined by in-situ measurements. We suggest that the Ni isotope variations and apparently heterogeneous initial ^{60}Fe/^{56}Fe results from physical sorting within the protosolar nebula of different phases (silicate, metal and sulphide) that carry different isotopic signatures.

1. Introduction

The relative abundances of the elements and their isotopes in the Solar System result from mixing in the protosolar nebula of material derived from different nucleosynthetic sources. Although various stellar components have been identified in individual pre-solar grains and refractory inclusions, the general absence of mass independent isotopic variability on the bulk meteorite scale bears testimony to the efficiency of nebular mixing. However, several studies have found non radiogenic, mass independent isotopic variations at the 0.1 ε unit (10 part-per-million) level in refractory elements in bulk meteorites (e.g. Niemeyer, 1985; Dauphas et al., 2002a; Yin et al., 2002; Andreasen and Sharma, 2006; Ranen and Jacobsen, 2006; Carlson et al., 2007; Trinquier et al., 2007). Such isotopic fingerprints are useful for examining the nucleosynthetic origins of Solar System material, relating differentiated and primitive meteorite types, and studying mixing processes in the early solar nebula.

Nickel is an attractive target for further study. It is a moderately refractory, moderately siderophile element, and is a major component of both iron and silicate meteorites. Ni has five stable isotopes (^{58}Ni, ^{60}Ni, ^{61}Ni, ^{62}Ni, ^{64}Ni), of which one (^{60}Ni) is the daughter of short-lived ^{60}Fe (half-life 1.49±0.27 Ma; Kutschera et al., 1984). Previous studies have found variations in the ^{62}Ni/^{61}Ni ratio of nucleosynthetic origin within calcium–aluminium inclusions (CAI) (Birck and Lugmair, 1988; Quitté et al., 2007). Ni isotope variations can therefore potentially be used both to trace constituent components in the nebula using stable ^{62}Ni and to date nebula events using radiogenic ^{60}Ni. Ni isotopes are thought to be dominantly produced by the nuclear statistical equilibrium process in a supernova environment, with different amounts of neutron enrichment influencing the relative proportions of heavy to light isotopes (Hartmann et al., 1985). Likewise, ^{60}Fe is believed to be synthesised in a high temperature stellar environment and not within or en route to the Solar System (e.g. Wasserburg et al., 1998; Gallino et al., 2004). The presence of live ^{60}Fe inferred from Ni isotope compositions represents a diagnostic fingerprint of material created in a nearby stellar explosion that was subsequently transported to the nascent solar nebula in <10 Ma. The initial abundance of ^{60}Fe, relative to other short-lived nuclides, can place important constraints on the nucleosynthetic processes responsible for creating these nuclides.

For these reasons, a number of studies have carried out Ni isotope measurements of meteorites and their components. Previous studies have reported mass dependent variations of up to 0.045% per atomic mass unit in the Ni isotope compositions of iron and chondritic meteorites (Moynier et al., 2007). Evidence for live ^{60}Fe has been found in

* Corresponding author. Department of Earth Sciences, Royal Holloway University of London, Egham, Surrey, TW20 0EX, UK. Tel.: +44 1784 443589; fax: +44 1784 471780.
E-mail address: m.regelous@gl.rhul.ac.uk (M. Regelous).

0012-821X/$ – see front matter © 2008 Elsevier B.V. All rights reserved.
doi:10.1016/j.epsl.2008.05.001

differentiated eucrite meteorites (Shukolyukov and Lugmair, 1993a,b) and in high Fe/Ni phases in primitive ordinary and enstatite chondrites (Tachibana and Huss, 2003; Mostefaoui et al., 2005; Tachibana et al., 2006; Guan et al., 2007), as well as excess ^{62}Ni in early-formed, calcium aluminium rich inclusions (Birck and Lugmair, 1988; Quitté et al., 2007). However, high precision Ni isotope measurements by MC-ICPMS have failed to show systematic differences of ^{60}Ni with Fe/Ni in iron meteorites (Cook et al., 2006; Quitté et al., 2006a; Bizzarro et al., 2007). This is unexpected, given the rapid timescales of planetesimal iron meteorite formation implied by W isotope studies (Kleine et al., 2005; Scherstén et al., 2006; Markowski et al., 2006a). For an initial Solar System ^{60}Fe/^{56}Fe ratio of ~5×10^{-7} (e.g. Tachibana et al., 2006), measurable differences in the radiogenic Ni isotope ratios of some iron meteorite groups are expected relative to a chondritic or terrestrial reference (Fig. 1). In addition, a recent study (Bizzarro et al., 2007) found negative ^{60}Ni anomalies in differentiated silicate meteorites (angrites) which have ancient model ages together with very high Fe/Ni, and are therefore expected to have large positive ^{60}Ni anomalies (Fig. 1).

In order to investigate these problematic observations, we have developed new procedures to measure Ni isotope ratios to higher precision than previously possible, and report here Ni isotope data for 11 magmatic iron and 13 chondritic meteorites.

2. Analytical techniques

2.1. Chemical separation and mass spectrometry procedures

Iron meteorites were leached in warm 6 M HCl for 10 min, in order to remove oxidised surfaces and possible terrestrial contamination. The weight loss during leaching was typically 5–10%. After rinsing in 18.2 MΩ/cm water, the remaining metal was dissolved completely in aqua regia. Silicate samples were dissolved in HF-HNO_3, treated with 15 M HNO_3 and 6 M HCl until the sample was completely in solution. Ni was separated from all samples using a three-stage ion exchange procedure which gave Ni yields within error of 100%. The first column separation uses a dimethylglyoxime (DMG) solution as a highly Ni-specific eluant and subsequent steps remove minor residual impurities. A detailed description of this procedure is provided in the Supplemental Data. Blanks for the entire process were between 5 and 15 ng, and are insignificant compared to the amounts of sample Ni processed (>20 μg).

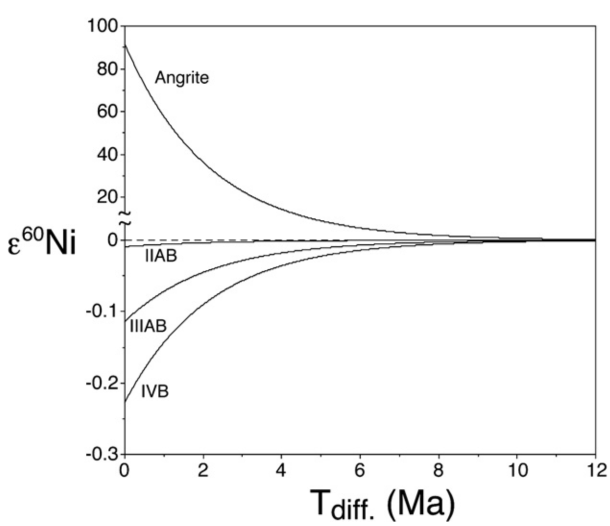

Fig. 1. Ni isotopic compositions predicted for IIAB, IIIAB, IVB iron meteorites and an angrite (differentiated silicate meteorite), for various ages of differentiation (T_{diff}) from a parent body with chondritic Fe/Ni (17.2), assuming an initial ^{60}Fe/^{56}Fe ratio of 5×10^{-7} (Tachibana et al., 2006), and a value of 4.621×10^{-7} a^{-1} for the ^{60}Fe decay constant. Ni isotopic compositions are expressed as ε^{60}Ni (the ^{60}Ni/^{61}Ni ratio expressed as parts per ten thousand difference relative to a terrestrial reference composition, which in this case is assumed to be the same as the chondritic parent, with an initial ^{60}Ni/^{61}Ni ratio of 23.0974). Positive anomalies of up to 90 ε^{60}Ni are expected for angrites with high Fe/Ni ratios of 5000, relative to chondrites or Earth (with ε^{60}Ni=0, as represented by the dashed line). In contrast, much smaller, negative ε^{60}Ni anomalies should characterise iron meteorites, which have variably low Fe/Ni ratios (averages taken as 16.7, 11.0 and 4.8 for IIAB, IIIAB and IVB respectively). Typical measurement precisions in this study are ±0.03 ε^{60}Ni. Note break in scale of *y*-axis at ε^{60}Ni=0.

Nickel isotope measurements were made using a ThermoFinnigan Neptune MC-ICPMS. Samples were dissolved in 0.3 M HNO_3 and introduced into the mass spectrometer via a Cetac Aridus desolvator. Measurements were made in 'medium resolution' mode (M/ΔM>6000 peak edge width from 5–95% full peak height). Mass 58 was measured on a Faraday cup connected to an amplifier with a 10^{10} Ω feedback resistor, enabling ^{58}Ni beams of ~900 pA to be measured. Each sample measurement was bracketed by measurements of the NIST SRM986 Ni isotope standard, and was typically measured 4 times in an analytical session. A mass bias correction was applied to the ^{62}Ni/^{61}Ni and ^{60}Ni/^{61}Ni ratios using the measured ^{61}Ni/^{58}Ni ratio and reference values from Gramlich et al. (1989). We used the ^{61}Ni/^{58}Ni ratio for normalisation, rather than ^{62}Ni/^{58}Ni, because mass independent Ni isotope variations previously documented in CAI have been interpreted in terms of variable contributions of the neutron-rich nuclides ^{62}Ni and ^{64}Ni (Birck and Lugmair, 1988; Quitté et al., 2007). Samples were further normalised to bracketing measurements of the SRM986 Ni standard. Ni isotope data are reported as ε^{60}Ni and ε^{62}Ni (the parts per ten thousand differences in ^{60}Ni/^{61}Ni and ^{62}Ni/^{61}Ni relative to the SRM986 standard, which is taken to represent the bulk Earth). The weighted means of multiple analyses of each sample and their standard errors (typically ±0.03 ε^{60}Ni and ±0.06 ε^{62}Ni, 2s.e., n=4) are reported in Table 1.

Fe/Ni ratios (Table 1) were measured on splits taken from sample solutions prior to the Ni separation, using a ThermoFinnigan Element 2 magnetic-sector ICP-MS (see Supplementary Data).

2.2. Evaluation of interference effects and accuracy

High precision isotope analyses using MC-ICPMS are potentially compromised by interferences on the masses of interest. Therefore, we carefully evaluated the possible effects of interferences on our Ni isotope measurements during each analytical session. Our separation chemistry very effectively removed sample matrix, which we quantified by magnetic sector ICP-MS analysis of the final Ni fractions (see Supplementary Data). Nevertheless, isobaric interferences that result from residual, minor Zn (<0.1 pA ^{64}Zn) and Fe (<0.05 pA ^{56}Fe) present in the Ni fractions need to be monitored. Since we were unable to measure simultaneously the entire mass range between ^{56}Fe and ^{66}Zn using our detector configuration, we chose to collect ^{56}Fe in order to correct accurately for the small interference of ^{58}Fe on ^{58}Ni. This meant that we were unable to correct measured ^{64}Ni intensities for the small but significant (<0.8%) ^{64}Zn interference, and ^{64}Ni data are therefore not reported in Table 1. It should be stressed that the correction on ^{58}Ni is very small, given the ^{58}Fe/^{58}Ni ratios of $<5\times10^{-6}$ determined for all our analyses.

The minor Ni background of our instrument (~0.02 pA of a typical 900 pA ^{58}Ni sample signal) was corrected for by measuring an on-peak zero before and after each sample measurement, whilst aspirating a solution of 0.3 M HNO_3. Possible molecular interferences were investigated by careful examination of mass-spectra using an electron multiplier in ion-counting mode. The most significant peak (~200 cps) was evident on the high mass shoulder of ^{62}Ni. We thus set our collectors to resolve ^{62}Ni from this peak (in addition to resolving ^{40}Ar^{16}O from the ^{56}Fe peak used for interference correction on ^{58}Ni). Interferences on other Ni peaks were still less significant (e.g. ^{40}Ar^{20}Ne, ^{40}Ar^{18}O) and deemed adequately corrected by our subtraction of on-peak zeros. Ca and Ti were not observed in the purified Ni fraction, and interferences of CaO^+ and TiO^+ species on Ni peaks were

Table 1
Ni isotope and supporting data for samples analysed in this study

Sample type	Sample name	Description	NHM number[a]	ε^{60}Ni[b]	±2 S.E.[c]	ε^{62}Ni[b]	±2 S.E.[c]	*n*[d]	Fe/Ni[e]	ε^{182}W[f]
Terrestrial standards										
	SRM986 col[g]	Ni metal		−0.006	0.026	0.010	0.048	8		
	JP-1	Peridotite		−0.001	0.014	0.030	0.020	*37*		
	BHVO-2	Basalt		−0.002	0.021	0.004	0.053	*8*		
	SRM361	Ni-rich steel		0.009	0.019	0.048	0.035	14		
Chondritic meteorites										
	Orgueil	CI	1985, M148	−0.004	0.027	0.253	0.048	8	15.8	
	Cold Bokkeveld	CM2	13989	−0.098	0.032	0.122	0.059	4	17.0	
	Murchison	CM2	1988, M23	−0.114	0.046	0.064	0.090	3	17.9	
	NWA 801	CR2		−0.216	0.044	0.071	0.078	4	18.4	
	Allende	CV3.2		−0.110	0.026	0.093	0.042	*10*	18.4	
	Leoville	CV3	1919, 144	−0.140	0.026	0.049	0.040	8	17.2	
	Felix	CO3.2	1919, 89	−0.068	0.032	0.125	0.051	6	16.9	
	Chainpur	LL3.3	1915, 86	−0.065	0.048	−0.072	0.090	3	16.2	
	Krymka	LL3.1	1956, 325	0.004	0.031	−0.089	0.074	4	20.0	
	Tieschitz	H/L3.6	1975, M11	−0.051	0.033	−0.035	0.058	4	13.0	
	Abee	EH4	992, M7	−0.017	0.047	−0.002	0.089	3	16.6	
	St. Mark's	EH5	1990, 339	−0.026	0.031	0.050	0.058	4	17.0	
	Khairpur	EL6	51366	−0.038	0.030	−0.054	0.054	4	24.8	
Iron meteorites										
	Arispe	IC	86,425	−0.051	0.027	−0.154	0.043	11	12.1	*−3.9*
	Bendegó	IC	66,585	0.021	0.027	−0.025	0.048	8	12.9	*−4.1*
	Coahuila	IIAB	54,242	−0.025	0.021	−0.123	0.039	11	16.7	−3.6
	Henbury	IIIAB		−0.061	0.037	−0.115	0.073	5	12.4	−3.7
	Lenarto	IIIAB	61,304	−0.060	0.029	−0.110	0.038	8	10.8	−3.4
	Bristol	IVA	1955, 226	−0.060	0.016	−0.056	0.035	20	11.3	−3.5
	Putnam	IVA	90,228	−0.116	0.047	−0.009	0.056	4	12.0	−3.5
	Cape of Good Hope	IVB	1985, M246	−0.159	0.025	0.126	0.038	8	5.2	−3.6
	Hoba	IVB	1930, 976	−0.120	0.015	0.073	0.026	*27*	5.1	−3.4
	Santa Clara	IVB	1983, M27	−0.162	0.037	0.174	0.056	4	4.7	−3.5
	Tlacotepec	IVB	1959, 913	−0.146	0.027	−0.005	0.042	8	5.2	*−4.1*

[a] Natural History Museum identification number.
[b] Weighted means of *n* individual Ni isotope analyses of each sample are reported in ε notation (see text).
[c] Uncertainties expressed as 2 standard errors (see Supplementary Data for full description of data treatment).
[d] Mean values that comprise individual measurements derived from full repeat dissolutions and sample processing highlighted with italics (in the case of Hoba multiple chemical processing of the same parent solution was undertaken, but no repeat dissolutions).
[e] Fe/Ni (elemental weight ratios) determined in this study for the meteoritic samples have a typical precision of 1% (see Supplementary Data).
[f] Tungsten isotope data for iron meteorites are listed for reference, as an indication of the influence of spallation. All tungsten data taken from Scherstén et al. (2006), except for Santa Clara (Markowski et al., 2006a). Samples that have ε^{182}W more negative than the initial ε^{182}W of the Solar System, −3.5±0.2 (Kleine et al., 2005) are clearly influenced by spallation and these values are italicised.
[g] NIST SRM986 col refers to a solution of the NBS986 Ni isotope standard that was processed through the chemical separation procedure used for samples, as opposed to the unprocessed solution used to bracket sample analyses (see Supplementary Data).

negligible. Any effects of irresolvable NiH^+ contributions to Ni^+ peaks were removed by normalising all sample data to values of bracketing measurements of the SRM986 standard. All sample and standard solutions measured in each analytical session were adjusted to have the same Ni concentration within ~5%, so that the magnitude of the correction for plasma-based interferences was the same in each case.

We analysed the Ni isotope composition of several terrestrial samples in order to check the accuracy of our measurements. We measured Ni separated from the NIST SRM361 steel standard, the peridotite standard JP-1, and the basalt standard BHVO-2, using the same chemical procedure used for meteorite samples. These terrestrial standards have Ni concentrations of between 2% and 119 ppm, and bulk compositions that span those of the meteorite samples analysed in this study. The mean Ni isotope ratios of these standards all yielded ε^{60}Ni and ε^{62}Ni values within 0.01 and 0.05 ε units respectively of the terrestrial SRM986 pure Ni standard (Table 1; see also Fig. A1, Supplementary Data). An aliquot of the SRM986 standard passed through the entire Ni separation procedure also yielded values within error of the unprocessed standard (Table 1). These results indicate that chemistry-, sample- and plasma-derived interferences and matrix effects are insignificant. Our total of 12 separate analyses (comprising four or more averaged individual measurements from a given analytical session) of the different terrestrial standards vary by ±0.06 ε^{60}Ni and ±0.08 ε^{62}Ni (2 standard deviations). This provides a conservative estimate of total procedural reproducibility, which takes into account the influence of different dissolutions, chemical separations and measurement sessions. These values are less than twice the 2 standard errors of the means from individual sessions and are in keeping with an additional assessment of the reproducibility of the dataset as a whole (see Supplementary Data).

3. Results

All but one of the iron meteorites analysed have Ni isotope compositions that are distinct from terrestrial Ni (Fig. 2a). ε^{60}Ni is negatively correlated with ε^{62}Ni in the iron meteorites, with IVB types lying at the low ε^{60}Ni, high ε^{62}Ni end of the array, whereas IIAB and IC irons define the high ε^{60}Ni, low ε^{62}Ni end (Fig. 2a). One sample (Bendegó, IC) is displaced from this array to higher ε^{60}Ni, close to the terrestrial value. There is a positive correlation between Fe/Ni and ε^{60}Ni, with IVB types having low ε^{60}Ni and low Fe/Ni (Fig. 3).

Chondrites have Ni isotope compositions which overlap the negative array defined by irons (Fig. 2). However, there are clear differences between carbonaceous chondrites, which have positive ε^{62}Ni values, and ordinary chondrites, which have $\varepsilon^{62}\text{Ni} < 1$. Of the chondrites we have analysed, only enstatite chondrites have average ε^{60}Ni and ε^{62}Ni

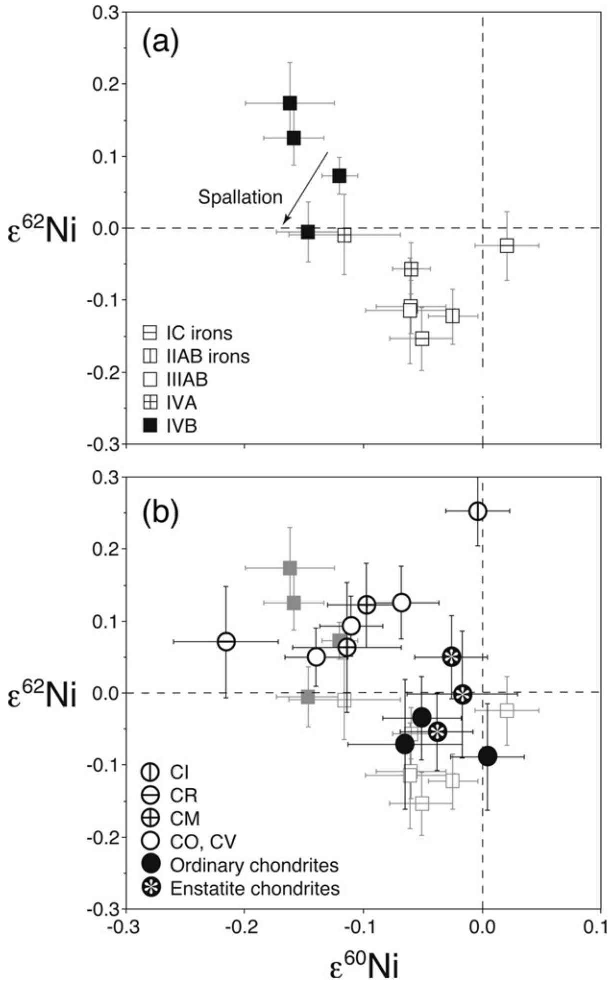

Fig. 2. Measured nickel isotope compositions of (a) iron and (b) chondritic meteorites analysed in this study. The iron meteorite data in (a) are shown for reference in (b) as grey symbols. The most common iron types (IIAB, IIIAB) have similar Ni isotope compositions to the most abundant (ordinary) chondrite types, and volatile-depleted IVB irons have ε^{60}Ni and ε^{62}Ni values that overlap with volatile-depleted CV, CO carbonaceous chondrites, which suggests that these iron and chondrite pairs may have accreted from material of similar composition. Of the chondrites, enstatite chondrites have the most similar Ni isotope compositions to the Earth. The likely influence of cosmic ray exposure on Ni isotope compositions is shown by the arrow in (a). This vector is calculated using the following mean thermal neutron capture cross sections (in barns), as taken from the Table of Nuclides website (http://atom.kaeri.re.kr/): ^{58}Ni, 30.8; ^{60}Ni, 4.32; ^{61}Ni, 11.24; ^{62}Ni, 23.7; ^{59}Co, 43.2. An elemental Ni/Co ratio of 20 was used for the calculation, taken to be representative of the IVB irons which have the oldest exposure ages and for which the influence of spallation will be most significant.

which overlap with the terrestrial values. In detail, ε^{60}Ni in carbonaceous chondrites appears positively correlated with ε^{62}Ni, with the one CI analysed in this study (Orgueil) lying at the high ε^{60}Ni end of this array.

Recently, Bizzarro et al. (2007) reported high precision Ni isotope measurements for a range of bulk meteorites that also show variable ε^{60}Ni and ε^{62}Ni. However, our data differ in several important respects. The iron meteorite data of Bizzarro et al. (2007) do not overlap with their chondrite data, and in addition show no variability in ε^{60}Ni or ε^{62}Ni. Since our study includes the same range of magmatic groups and even some of the same meteorite samples, the contrasting results presumably reflect analytical biases. We suggest that the iron meteorite data of Bizzarro et al. (2007) may be compromised by an interference on mass 61 (see further discussion in the Supplementary Data). The combination of our highly selective Ni separation chemistry coupled with analysis of much larger accumulated ion currents gives us confidence in the accuracy of our results.

4. Discussion

4.1. Influence of spallation

An important issue that must first be addressed is the possible influence of cosmic ray induced spallation. Spallogenic neutrons may have modified the Ni isotope compositions of our samples, particularly the iron meteorites, which typically have long exposure ages. Such effects vary with exposure age and depth of the sample within the meteorite. Although exposure ages are known for the majority of the irons we have studied, we have no information on the location of our sample fragments relative to the original surface. However, an independent monitor of secondary neutron capture reactions is provided by the W isotope ratios of our samples. It has been shown that values of ε^{182} W lower than that of the initial Solar System indicate significant perturbation by spallation (Scherstén et al., 2006; Markowski et al., 2006b). Since only three of our samples have such a signature (Table 1), and because neutron capture cross sections of Ni isotopes are small compared to those of W, the overall importance of spallation on the Ni isotope variation is likely to be minor for most samples. Most of the samples analysed in this study were from the same meteorite fragments analysed by Scherstén et al. (2006), so the literature W isotope ratios provide a valuable monitor of spallation influence.

Our sample of Tlacotepec, however, has a markedly negative W isotopic signature (Table 1). It also has ε^{62}Ni significantly lower than our other three group IVB samples (Fig. 2a), which have unperturbed W isotope ratios (Table 1). Fig. 2a shows that the offset of Tlacotepec from the other Group IVB irons is consistent with a vector of spallogenic influence calculated using mean thermal neutron capture cross-sections. Our only other samples with spallation-affected W isotope ratios are the two group IC meteorites (Table 1). Despite being from the same magmatic group, these two IC samples have Ni isotopic ratios distinct from one another (Fig. 2a). This may partially reflect the consequences of spallation, although both have similarly perturbed W

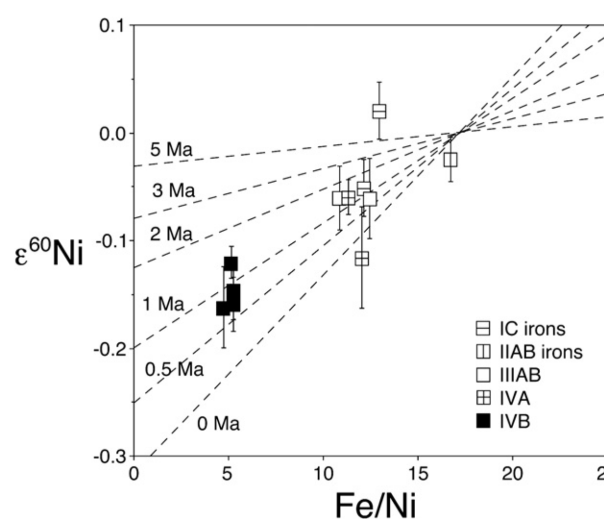

Fig. 3. Variation of ε^{60}Ni with Fe/Ni for iron meteorites analysed in this study. Dashed lines show ε^{60}Ni values expected for a given Fe/Ni ratio, for ages of differentiation of between 0 and 5 Ma after CAI formation, assuming an initially chondritic parent with Fe/Ni = 17.2 and an initial ^{60}Fe/^{56}Fe ratio of 5×10^{-7}. The broad positive array defined by iron meteorites could be explained by decay of live ^{60}Fe if metal segregation in iron parent bodies occurred within ~1 Ma of CAI formation, as implied by W isotope data (Kleine et al., 2005; Scherstén et al., 2006). However, Fig. 2b shows that chondrites have a similar range in ε^{60}Ni to irons, despite a much smaller range in Fe/Ni, indicating that much of the observed variation in ε^{60}Ni may not be the result of decay of live ^{60}Fe.

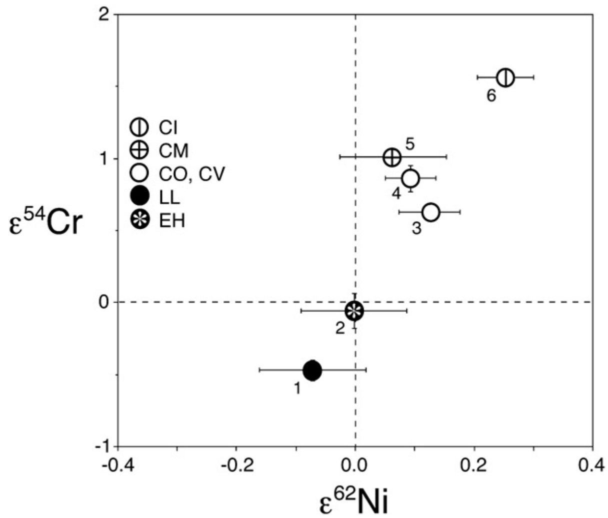

Fig. 4. ε^{62}Ni and ε^{54}Cr for individual chondrites which have been analysed for both isotope systems (Cr isotope data from Trinquier et al., 2007). Neutron-rich ^{54}Cr and ^{62}Ni are likely to be produced together in stars, and the positive correlation in bulk chondrites could be explained by incomplete mixing of a high ε^{62}Ni, high ε^{54}Cr component, most likely contained in a silicate phase, and a low ε^{62}Ni, low ε^{54}Cr component, inferred to be contained in a metal phase (see text for discussion). Note that enstatite chondrites have Ni and Cr isotope compositions similar to Earth. Sample names: 1, Chainpur (LL3.4); 2, Abee (EH4); 3, Felix (CO3), 4, Allende (CV3); 5, Murchison (CM2); Orgueil (CI1).

isotope ratios. It is therefore perhaps more likely that Arispe, with its anomalous Ir content (Scott, 1977), is not cogenetic with other IC meteorites.

Chondrites have much younger exposure ages than irons, and spallation effects on Ni isotopes are therefore expected to be negligible for these samples.

4.2. Origin of Ni isotope variations in meteorites

The magmatic iron meteorites analysed in this study span a wide range of Fe/Ni, from ~5 in the group IVB to ~17 in group IIAB. If iron meteorites formed within ~1 Ma of the earliest dated Solar System solids, as implied by recent high-precision W isotope data (Kleine et al., 2005; Markowski et al., 2006b; Scherstén et al., 2006), and if live ^{60}Fe was present at this time, then irons would be expected to have negative ε^{60}Ni, with the most negative values in the IVB samples with the lowest Fe/Ni (Fig. 1). Fig. 3 shows that the variation in ε^{60}Ni within the iron meteorite samples are indeed positively correlated with variations in Fe/Ni, and that the observed range in ε^{60}Ni is apparently consistent with early core segregation in iron parent bodies (within 0.5–1.0 Ma of CAI), assuming a Solar System initial ^{60}Fe/^{56}Fe ratio of 5×10^{-7} (Tachibana et al., 2006). However, as is evident from Fig. 2a, ε^{60}Ni values are also inversely correlated with ε^{62}Ni. Differences in ε^{62}Ni are not the result of radioactive decay and so the cause of the arrays in Figs. 2a and 3 needs further explanation.

Fig. 2b shows that chondrites have variations in ε^{60}Ni as large as those in irons. In addition, the Ni isotope compositions of chondritic and iron meteorites largely overlap, with only the CI chondrite being clearly distinct (Fig. 2b). Since chondrites all have similar Fe/Ni, no relative differences in Ni isotope ratios will be imparted by decay of ^{60}Fe (as long as ^{60}Fe was homogenously distributed in the Solar System). The correlation of ε^{60}Ni and ε^{62}Ni in irons likewise suggests that their ^{60}Ni/^{61}Ni variations are associated with inherited differences in ^{62}Ni/^{61}Ni, rather than variable contributions from the decay of live ^{60}Fe. We therefore first examine the role of nucleosynthetic variations on the Ni isotope compositions of our samples, before assessing the role of decay of ^{60}Fe.

4.3. Ni isotope variations of nucleosynthetic origin

There is a ~0.4 ε unit variation in ^{62}Ni/^{61}Ni within our sample suite as a whole. Since spallation processes appear not to have influenced the nickel isotope compositions of most of the samples we have analysed, the variation in ε^{62}Ni within these samples is likely to be of nucleosynthetic origin. This conclusion is supported by published ^{54}Cr isotope data (Trinquier et al., 2007). Both ^{62}Ni and ^{54}Cr are neutron-rich nuclides of iron-peak elements, and these two isotopes are expected to be co-produced during nucleosynthesis. There is a positive correlation between ε^{54}Cr and ε^{62}Ni (Fig. 4) for individual chondritic meteorites that have been analysed for both ^{54}Cr (Trinquier et al., 2007) and ^{62}Ni (this study). Carbonaceous chondrites have positive ε^{54}Cr and ε^{62}Ni whereas ordinary chondrites have negative ε^{62}Ni and ε^{54}Cr. The only chondrites that clearly have the same Ni isotopic composition as the Earth are the enstatite chondrites, which also have ε^{54}Cr values of zero (Trinquier et al., 2007).

We interpret the Ni isotope variations within chondrites as the result of incomplete mixing of various Ni-bearing phases of different nucleosynthetic origin. At least three distinct components are required to explain the observed Ni isotope variations. The carbonaceous chondrites appear to define an array of increasing ε^{60}Ni and ε^{62}Ni towards CI (Fig. 2b). As is evident in Fig. 5, this array extends towards the much more extreme compositions represented by some CAI (Quitté et al., 2007). However, since the CAI-rich CO/CV chondrites do not have the highest ε^{60}Ni and ε^{62}Ni, the high ε^{62}Ni component cannot be CAI alone (and CAI are in any case highly heterogeneous). Stepwise leaching of CI chondrites has shown that neutron-rich ^{54}Cr (and by implication ^{62}Ni) is apparently carried in a more widely dispersed silicate phase in the least metamorphosed carbonaceous chondrite types (Rotaru et al., 1992; Shukolyukov and Lugmair, 2006; Trinquier et al., 2007), and in some cases also in an unidentified, HCl-soluble phase (Podosek et al., 1997).

Within carbonaceous chondrites, high ε^{62}Ni is associated with high ε^{60}Ni. The nucleosynthetic processes that produce abundant ^{62}Ni are not also expected to over-produce ^{60}Ni, but could produce neutron-rich ^{60}Fe (e.g. Quitté et al., 2007). The high ^{60}Ni component most evident in CI may therefore represent either 'fossil' ^{60}Fe, created in earlier nucleosynthetic events, or live ^{60}Fe. In the latter case, meteorites derived from differentiated planetesimals built from similar

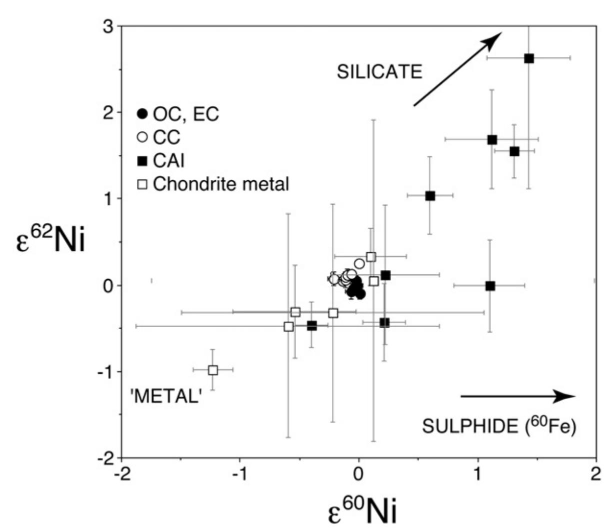

Fig. 5. Nickel isotope compositions of iron and chondritic meteorites (data from this study), bulk CAI (Quitté et al., 2007) and chondrite metal (Cook et al., 2006). An arrow indicates very high ε^{60}Ni values of some sulphides (>100), for which no ^{62}Ni/^{61}Ni data have been reported. The Ni isotope variations observed in bulk chondrites can be explained by mixing of at least three components with distinct Ni compositions, as discussed in the text.

precursor materials to carbonaceous chondrites might be expected to preserve variations in radiogenic ^{60}Ni, and this is discussed further below.

Several lines of evidence suggest that the low $\varepsilon^{60}Ni$, low $\varepsilon^{62}Ni$ component in carbonaceous chondrites is contained in a metal phase, which contains a large proportion of the Fe and Ni budget of most chondrites. Leaching experiments carried out on unmetamorphosed carbonaceous chondrites (Trinquier et al., 2007) show that the leach fraction corresponding to metal has low $\varepsilon^{54}Cr$ (and presumably low $\varepsilon^{62}Ni$). In addition, metal separated from chondritic meteorites is characterised by low $\varepsilon^{60}Ni$ and $\varepsilon^{62}Ni$ (Cook et al., 2006). Despite the poorer precision (~0.15ε) of these analyses, metal separates from Semarkona (an unequilibrated ordinary chondrite) showed resolvably positive $\varepsilon^{61}Ni$ (Cook et al., 2006), which corresponds to negative $\varepsilon^{62}Ni$ (~−1.0) using the normalisation scheme of our study (Fig. 5). Additional high precision Ni isotope analyses of metal separates from relatively unmetamorphosed carbonaceous chondrites are needed to confirm these findings.

Mass-independent isotopic variability in refractory and moderately refractory elements were first identified in CAI (see review in Birck, 2004), but were subsequently found in more muted form in bulk samples (e.g. Niemeyer, 1985). More recently, ppm-level mass-independent isotopic variations in a wider range of elements have been reported, although some of the observations and interpretations remain contentious (see summary in Leya et al., 2008). It has been suggested that the distinctive isotope compositions of some elements in bulk carbonaceous chondrites may result from incomplete sample dissolution, leaving residual pre-solar grains (e.g. Yokoyama et al., 2007; Carlson et al., 2007). Although our digestion procedure will not have fully dissolved rare, refractory presolar phases such as SiC in carbonaceous chondrite samples, the abundance of Ni in presolar grains is unlikely to be high enough (Kashiv et al., 2001) for this to influence the measured Ni isotope compositions. In addition, the range in $\varepsilon^{62}Ni$ that we find in irons is highly unlikely to result from incomplete sample dissolution.

It has also recently been suggested that mass independent isotopic variations observed in a number of elements in some CAI is the result of fractionations within the Solar System, controlled by differences in nuclear radii rather than inherited from contrasting nucleosynthetic processes (Fujii et al., 2006). Such a process would result in larger variations in $^{62}Ni/^{61}Ni$ (normalised to $^{58}Ni/^{61}Ni$), as used throughout this study, compared to $^{58}Ni/^{60}Ni$ (normalised to $^{62}Ni/^{60}Ni$), since the latter scheme contains no odd-mass nuclide with contrasting nuclear radius. As can be seen in Fig. 6, this is not the case, and so we believe that nuclear radius effects do not have a significant influence on our Ni isotope variation.

In summary, the observed range in $\varepsilon^{62}Ni$ could be explained by variable mixing of a rare high $\varepsilon^{62}Ni$, high $\varepsilon^{60}Ni$ silicate phase with a low $\varepsilon^{62}Ni$, low $\varepsilon^{60}Ni$ reservoir, possibly contained in metal. Additional variability of $\varepsilon^{60}Ni$ at a given $\varepsilon^{62}Ni$ in our samples (Fig. 2) and in CAI (Fig. 5) may be the result of heterogenous distribution of either live ^{60}Fe, or 'fossil' ^{60}Fe in the form of radiogenic ^{60}Ni. In-situ measurements of ordinary and enstatite chondrites show that sulphide phases with high Fe/Ni ratios are characterised by high $\varepsilon^{60}Ni$. Whether or not the elevated ^{60}Fe in these sulphides, and in the high $\varepsilon^{60}Ni$ silicate phase was live at the time of accretion of the solar nebula is discussed in more detail in Section 4.5.

4.4. Linking precursor material to differentiated and primitive meteorite types

Mass independent variations in oxygen isotopes are widely used to fingerprint the provenance of meteorites (e.g. Clayton, 2004). For iron meteorites however, this approach can only be used in the case of rare samples which contain phosphate, chromite or silicate inclusions. In addition, mass independent variations in the O isotope compositions

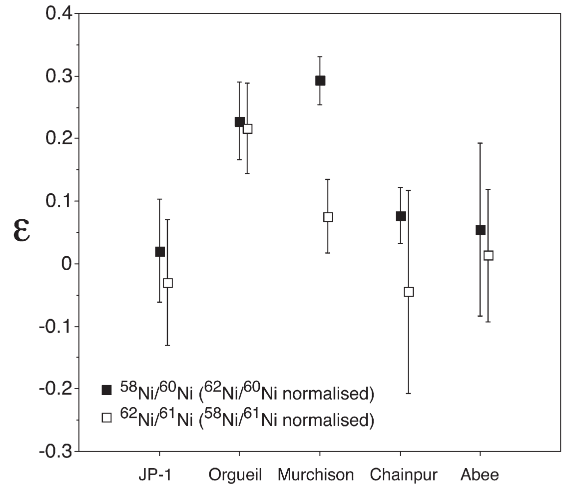

Fig. 6. Data for a single run including a full compositional range of meteorites, with nickel isotope data reported as $^{62}Ni/^{61}Ni$ normalised to $^{58}Ni/^{61}Ni$ (as in the rest of this study), and $^{58}Ni/^{60}Ni$ normalised to $^{62}Ni/^{60}Ni$. The latter scheme involves all even nuclides of comparable radii, and so should show minor variability if nuclear radii play an important role in controlling isotopic variability. This is clearly not the case. Errors are larger than reported in Table 1, as the data are from a single run, rather than averages of all runs over the period of study.

of meteorites are thought to result largely from photo-disassociation reactions occurring in the gas phase (Clayton, 2002) that are subsequently imparted to solids. Recent models of these processes suggest that O isotope compositions will vary with both time and radial position in the protosolar nebula (Yurimoto and Kuramoto, 2004; Krot et al., 2005; Lyons and Young, 2005). Oxygen isotope signatures may therefore not uniquely characterise material that aggregated to form meteorite parent bodies, and likely reflect local, Solar System processes rather than mixing of pre-solar components. In contrast, $\varepsilon^{62}Ni$ variations appear to be primarily the result of incomplete mixing of different nucleosynthetic components within the nebula. Nickel isotope variations should therefore provide valuable complementary information to the oxygen isotope system, by tracing the pre-solar origin of the materials that make up both chondritic and differentiated (including iron) meteorites.

As shown above, the Ni isotope compositions of iron and chondritic meteorites largely overlap (Fig. 2), suggesting that the planetesimals from which both were derived aggregated from precursor material of similar composition. In detail, both the IVB iron meteorites and the CM, CO and CV carbonaceous chondrites have negative $\varepsilon^{60}Ni$ and positive $\varepsilon^{62}Ni$. Intriguingly, the low Ge IVB irons and the low Mg/Al CV and CO carbonaceous chondrites are both volatile depleted and this, together with their common Ni isotopic signatures, suggests that they may be derived from parent bodies which accreted from material with similar isotopic and chemical composition.

The other magmatic iron meteorite groups studied (excluding one IVA sample with large errors) are distinct from carbonaceous chondrites and more similar to ordinary chondrites. Given the small range in Ni isotope compositions, it is difficult to make a more detailed comparison. The similarity of $\varepsilon^{62}Ni$ in LL chondrites and IVA irons is consistent with oxygen isotope measurements (e.g. Clayton and Mayeda, 1996). On the other hand, IIAB and IIIAB irons also have $\varepsilon^{62}Ni$ values that overlap with ordinary chondrites, in apparent conflict with O isotope evidence; ordinary chondrites lie above the terrestrial fractionation line (TFL) in O isotope space, whereas phosphates and chromites in IIIAB lie below the TFL (e.g. Clayton and Mayeda, 1996). Further work is required to determine whether or not significant differences between these groups can be resolved. As discussed above however, the O isotope composition of material within the protosolar nebula likely varied both temporally and spatially, so that O isotope variations need not be coupled to the isotopic composition of non-volatile elements in the precursor materials to different planetesimals.

Of the elements for which nucleosynthetic variations have been detected in bulk meteorites, only Ni is present at concentrations of >100 ppm in almost all meteorite types. Our approach can therefore be extended to other meteorite types, in particular differentiated silicate meteorites such as angrites and eucrites. Nucleosynthetic variations in ^{54}Cr in bulk chondrites are somewhat larger than those in ^{62}Ni (Trinquier et al., 2007), but accurate Cr isotope measurements can only be easily obtained for silicate meteorite types, since some irons contain little Cr, and spallation production of Cr from Fe compromises bulk analysis. In contrast, Ni isotopes can fingerprint the provenance of a major, non-volatile component of all meteorite types.

Of the chondrite types analysed in this study, only enstatite chondrites have Ni isotope compositions that are identical to that of Earth (Fig. 2b). Previous studies have shown that the O, Cr and Mo isotope compositions of enstatite chondrites are also identical to those of the Earth (Dauphas et al., 2002b; Clayton, 2004; Trinquier et al., 2007). Our data therefore support previous suggestions (e.g. Javoy and Pineau, 1983) that enstatite chondrites represent the most suitable proxy for the bulk Earth composition. There are apparent elemental mass balance problems that result from constructing the Earth from enstatite chondrites, but this could reflect element fractionation during planetary accretion and differentiation (Javoy, 1995). Thus the mismatch between the sampled terrestrial silicate reservoirs and enstatite chondrites may give insights into the early processes that shaped the Earth. For example, difficulties in making the Earth's mantle from a silica rich and highly reduced protolith could be explained by incorporation of Si into the core (Takafuji et al., 2005; Georg et al., 2007) and subsequent mantle oxidation by perovskite disproportionation (Wade and Wood, 2005).

4.5. Live ^{60}Fe in the early Solar System?

The ^{60}Fe–^{60}Ni system is potentially a useful short-lived chronometer for dating events within the first ~10 Ma of Solar System history. The initial abundance of ^{60}Fe in the solar nebula is an important constraint on models for the stellar nucleosynthesis of short-lived radionuclides, which in turn has implications for the trigger for nebula collapse. Unfortunately, the initial ^{60}Fe/^{56}Fe ratio of the Solar System is at present not well constrained. Ni isotope data for eucrites with high Fe/Ni give varying estimates for ^{60}Fe/^{56}Fe of $3.9\pm0.6\times10^{-9}$ to $4.3\pm1.5\times10^{-10}$, probably as a result of secondary disturbance (Shukolyukov and Lugmair, 1993a,b). In-situ Ni isotope analyses of sulphides in ordinary chondrites yield ^{60}Fe/^{56}Fe in the range $1.08\pm0.23\times10^{-7}$ to $0.92\pm0.24\times10^{-6}$ (Tachibana and Huss, 2003; Mostefaoui et al., 2004, 2005), similar to estimates from sulphides in enstatite chondrites (Guan et al., 2007). The age of formation of these sulphides is not known precisely, and so better constraints on the initial ^{60}Fe/^{56}Fe may be obtained from chondrules and their inclusions. Ni isotope compositions of bulk chondrules from Allende (CV3) and Tieschitz (H3.6) do not yield clear evidence for live ^{60}Fe, possibly due to redistribution of Ni during metamorphism (Quitté et al., 2006b). Two recent ion-microprobe studies of chondrules and inclusions from unequilibrated ordinary chondrites (Tachibana et al., 2006; Goswami et al., 2007) yielded estimates of $5–10\times10^{-7}$ and $2.3\pm1.8\times10^{-6}$ for the initial ^{60}Fe/^{56}Fe ratio of the Solar System.

If magmatic iron and chondritic meteorites with the same ε^{62}Ni were derived from similar precursor material, as argued above, then our data can be used to place some constraints on the ^{60}Fe/^{56}Fe ratio at the time of metal segregation. Group IIAB irons have near-chondritic Fe/Ni ratios (average ~16.7) and so are predicted to develop an irresolvable <0.01 ε^{60}Ni deficit relative to ordinary chondrites with Fe/Ni=17.2, assuming an initial ^{60}Fe/^{56}Fe ~5×10^{-7} (Tachibana et al., 2006) and core segregation at 1 Ma after CAI formation (see Fig. 1). This is consistent with our observations, since ε^{60}Ni values of OC and IIAB are the same within error. A larger (~0.07) deficit in ε^{60}Ni relative to ordinary chondrites is predicted for IIIAB (or IVA) irons (Fig. 1), but this is not apparent in our data (Fig. 2). Our results thus do not clearly support the higher estimates (>5×10^{-7}) of initial ^{60}Fe/^{56}Fe in ordinary chondrites, but could be consistent with an initial ^{60}Fe/^{56}Fe of less than 3×10^{-7} (leading to a ε^{60}Ni deficit of below ~0.03 in IIIAB) which is within the current range of estimates.

If the low Fe/Ni (~4.8) IVB irons and CO, CV carbonaceous chondrites were derived from similar precursor material as implied by their similar ε^{62}Ni, then assuming an initial ^{60}Fe/^{56}Fe of 5×10^{-7} and that metal segregation took place 1 Ma after CAI formation, we would predict a 0.14 deficit in ε^{60}Ni in the former compared to the latter (Fig. 1), which is not observed (Fig. 2b). We infer that carbonaceous chondrites must have had initial ^{60}Fe/^{56}Fe <1×10^{-7}. This contrasts with the higher values that apparently characterise ordinary and enstatite chondrites (Tachibana and Huss, 2003; Mostefaoui et al., 2005; Tachibana et al., 2006; Guan et al., 2007), and have been inferred for carbonaceous chondrites (Quitté et al., 2007).

There are several possible solutions to this dilemma, although in each case the use of the ^{60}Fe–^{60}Ni system as a chronometer is compromised. Bizzarro et al. (2007) suggested that ^{60}Fe was injected late into the nebula after the formation of differentiated bodies, in order to explain the lack of very positive ε^{60}Ni in ancient differentiated silicate meteorites (angrites) with very high Fe/Ni. However, if the parent bodies of irons differentiated prior to chondrite accretion (Kleine et al., 2005; Markowski et al., 2006a; Scherstén et al., 2006), this model would predict systematic differences in ε^{60}Ni between chondrites and iron meteorites. Although Bizzarro et al. (2007) reported such a contrast, we believe this result may be an analytical artifact (see Supplementary Data), and we do not see this feature in our dataset (Fig. 2).

Alternatively, heterogeneity in ^{60}Fe may be spatial rather than temporal. Spatial heterogeneity in ^{53}Mn has been proposed to explain an apparent heliocentric variation in the initial ^{53}Mn/^{55}Mn (Lugmair and Shukolyukov, 1998). However, it is possible that variations in initial ^{53}Mn/^{55}Mn inferred from ^{53}Cr/^{52}Cr data in fact result from variation in ^{54}Cr/^{52}Cr in bulk meteorites (Trinquier et al., 2007), since this ratio was used for normalisation of the Cr isotope data in earlier studies (Lugmair and Shukolyukov, 1998). Our results suggest that carbonaceous chondrites may have formed in a region that accreted little live ^{60}Fe, and this hypothesis could be tested by in-situ Ni isotope measurements of high Fe/Ni phases in carbonaceous chondrites. The higher ε^{60}Ni of ordinary chondrites relative to carbonaceous chondrites could then be accounted for by the decay of an initial ^{60}Fe/^{56}Fe ~3×10^{-7} in the former compared to 1×10^{-7} in the latter, given an initial single ε^{60}Ni–ε^{62}Ni array with positive slope for chondritic meteorites.

In summary, our data appear to require initial ^{60}Fe/^{56}Fe ratios of <1×10^{-7} in carbonaceous chondrites. An initial ^{60}Fe/^{56}Fe ratio as high as 3×10^{-7} could characterise ordinary and enstatite chondrites, consistent with in-situ studies, but such high values are not demanded by our data. Further work is required to resolve the apparent discrepancies between bulk (Quitté et al., 2006) and in-situ (Tachibana and Huss, 2003; Mostefaoui et al., 2005; Tachibana et al., 2006) determinations of initial ^{60}Fe/^{56}Fe made on, admittedly different, ordinary chondrites.

The inferred inhomogenous distribution of ^{60}Fe contrasts with the apparently highly uniform distribution of ^{26}Al within the solar nebula (e.g. McKeegan and Davies, 2004). However live ^{60}Fe was apparently carried in a sulphide phase (Tachibana and Huss, 2003; Mostefaoui et al., 2005; Guan et al., 2007) whereas live ^{26}Al will have been hosted in a silicate phase. Differential sorting of silicates and sulphides can lead to decoupling of these systems. Similarly, physical separation of silicate and metal phases, with high ^{62}Ni and low ^{62}Ni respectively, may account for ^{62}Ni heterogeneity in the solar nebula.

5. Conclusions

Our new high-precision Ni isotope measurements show that there are small but significant variations in the $^{60}Ni/^{61}Ni$ and $^{62}Ni/^{61}Ni$ ratios in bulk iron ($\varepsilon^{60}Ni$ −0.16 to 0.02, $\varepsilon^{62}Ni$ −0.15 to 0.17 respectively) and chondritic meteorites (−0.22 to 0.00, −0.09 to 0.25). Only enstatite chondrites have identical Ni isotope compositions to Earth. Variations in $\varepsilon^{62}Ni$ are of nucleosynthetic origin and provide a means to link chondritic and differentiated meteorite types, using a moderately refractory major element. Based on their similar Ni isotope compositions, Group IVB irons and CO, CV carbonaceous chondrites may have accreted from precursor material of similar isotopic composition. Similarly, the overlap in Ni isotope composition between the abundant IIAB/IIIAB/IVA magmatic irons and ordinary chondrites suggests that these were also derived from precursor material of similar composition. Variations in $\varepsilon^{62}Ni$ between different chondrites are positively correlated with $\varepsilon^{54}Cr$, suggesting heterogeneous distribution in the nebula of a pre-solar phase (likely silicate) containing high abundances of neutron-rich iron-peak nuclides. At least some of the variability in $\varepsilon^{60}Ni$ within carbonaceous chondrites may result from variable 'fossil' ^{60}Fe associated with this high ^{62}Ni, high ^{54}Cr phase. If the parent bodies of IVB and CO, CV chondrites, and also II/IIIAB/IVA and ordinary chondrites were built from precursor material of similar isotopic composition, then the overlap in $\varepsilon^{60}Ni$ can be used to place upper limits on the $^{60}Fe/^{56}Fe$ of this material. Initial $^{60}Fe/^{56}Fe$ ratios as high as 3×10^{-7} may characterise ordinary chondrites, consistent with existing Ni isotope data for sulphides in ordinary chondrites. However carbonaceous chondrites would have to have $^{60}Fe/^{56}Fe < 1\times10^{-7}$, implying that ^{60}Fe was not homogenously distributed in the early solar nebula.

Acknowledgments

We thank Sara Russell and Caroline Smith (Natural History Museum) for advice, encouragement and meteorite samples. We are grateful for two anonymous reviews and the swift and helpful editorial handling of Rick Carlson. This work was funded by NERC GR3/JIF/46.

Appendix A. Supplementary data

Supplementary data associated with this article can be found, in the online version, at doi:10.1016/j.epsl.2008.05.001.

References

Andreasen, R., Sharma, M., 2006. Solar nebula heterogeneity in p-process samarium and neodymium isotopes. Science 314, 806–809.
Birck, J.-L., 2004. An overview of isotopic anomalies in extraterrestrial materials and their nucleosynthetic heritage. Rev. Mineral. Geochem. 55, 25–64.
Birck, J.-L., Lugmair, G.W., 1988. Nickel and chromium isotopes in Allende inclusions. Earth Planet. Sci. Lett. 90, 131–143.
Bizzarro, M., Ulfbeck, D., Trinquier, A., Thrane, K., Connelly, J.N., Meyer, B.S., 2007. Evidence for a late supernova injection of ^{60}Fe into the protoplanetary disk. Science 316, 1178–1181.
Carlson, R.W., Boyet, M., Horan, M., 2007. Chondrite barium, neodymium and samarium isotopic heterogeneity and early Earth differentiation. Science 316, 1175–1178.
Clayton, R.N., 2002. Self-shielding in the solar nebula. Nature 415, 860–861.
Clayton, R.N., 2004. Oxygen isotopes in meteorites. Treatise Geochem. 1, 129–142.
Clayton, R.N., Mayeda, T.K., 1996. Oxygen isotope studies of achondrites. Geochim. Cosmochim. Acta 60, 1999–2017.
Cook, D.L., Wadhwa, M., Janney, P.E., Dauphas, N., Clayton, R.N., Davis, A.M., 2006. High-precision measurements of non mass dependent effects in nickel isotopes in meteoritic metal via multicollector ICPMS. Anal. Chem. 78, 8477–8484.
Dauphas, N., Marty, B., Reisberg, L., 2002a. Molybdenum evidence for inherited planetary scale isotope heterogeneity of the protosolar nebula. Astrophys. J. 565, 640–644.
Dauphas, N., Marty, B., Reisberg, L., 2002b. Inference on terrestrial genesis from molybdenum isotope systematics. Geophys. Res. Lett. 29. doi:10.1029/2001GL014237.
Fujii, T., Moynier, F., Albarède, F., 2006. Nuclear field vs. nucleosynthetic effects as cause of isotopic anomalies in the early Solar System. Earth Planet. Sci. Lett. 247, 1–9.
Gallino, R., Busso, M., Wasserburg, G.J., Straniero, O., 2004. Early Solar System radioactivity and AGB stars. New Astron. Rev. 48, 133–138.
Georg, R.B., Halliday, A.N., Schauble, E.A., Reynolds, B.C., 2007. Silicon in the Earth's core. Nature 447, 1102–1106.
Goswami, J.N., Mishra, R., Rudraswami, N.G., 2007. ^{60}Fe and ^{26}Al records in chondrules from unequilibrated ordinary chondrites of low petrologic type. Lunar Planet. Sci. XXXVIII abstract 1943.
Gramlich, J.W., Machlan, L.A., Barnes, I.L., Paulsen, P.J., 1989. Absolute isotopic abundance ratios and atomic weight of a reference sample of nickel. J. Res. N.I.S.T. 94, 347–356.
Guan, Y., Huss, G.R., Leshin, L.A., 2007. ^{60}Fe–^{60}Ni and ^{53}Mn–^{53}Cr isotopic systems in sulfides from unequilibrated enstatite chondrites. Geochim. Cosmochim. Acta 71, 4082–4091.
Hartmann, D., Woosley, S.E., El Eid, M.F., 1985. Nucleosynthesis in neutron-rich supernova ejecta. Astrophys. J. 297, 837–845.
Javoy, M., 1995. The integral enstatite chondrite model of the Earth. Geophys. Res. Lett. 22, 2219–2222.
Javoy, M., Pineau, F., 1983. Stable isotope constraints on a model Earth from a study of mantle nitrogen. Meteoritics 18, 320–321.
Kashiv, Y., Cai, Z., Lai, B., Sutton, S.R., Lewis, R.S., Davis, A.M., Clayton, R.N., Pellin, M.J., 2001. Synchrotron X-ray fluorescence: a new approach for determining trace element concentrations in individual presolar SiC grains. Lunar Planet. Sci. XXXII, 2192 (abstract).
Kleine, T., Mezger, K., Palme, H., Scherer, E., Münker, C., 2005. Early core formation in asteroids and late accretion of chondrite parent bodies: evidence from ^{182}Hf–^{182}W in CAIs, metal-rich chondrites, and iron meteorites. Geochim. Cosmochim. Acta 69, 5805–5818.
Krot, A.N., Hutcheon, I.D., Yurimoto, H., Cuzzi, J.N., McKeegan, K.D., Scott, E.R.D., Libourel, G., Chassidon, M., Aleon, J., Petaev, M.I., 2005. Evolution of oxygen isotopic composition in the inner solar nebula. Astrophys. J. 622, 1333–1342.
Kutschera, W., Billquist, P.J., Frekers, D., Hemming, W., Jensen, K.J., Xiuzeng, M., Pardo, R., Paul, M., Rehm, K.E., Smither, R.K., Yntema, J.L., Mausner, L.F., 1984. Half-life of ^{60}Fe. Nucl. Instrum. Methods Phys. Res. B5, 430–435.
Leya, I., Schönbächler, M., Wiechert, U., Krähenbühl, U., Halliday, A.N., 2008. Titanium isotopes and the radial heterogeneity of the Solar System. Earth Planet. Sci. Lett. 266, 233–244.
Lugmair, G.W., Shukolyukov, A., 1998. Early Solar System timescales according to ^{53}Mn–^{53}Cr systematics. Geochim. Cosmochim. Acta 62, 2863–2886.
Lyons, J.R., Young, E.D., 2005. CO self-shielding as the origin of oxygen isotope anomalies in the early solar nebula. Nature 435, 317–320.
Markowski, A., Quitté, G., Halliday, A.N., Kleine, T., 2006a. Tungsten isotopic compositions of iron meteorites: chronological constraints vs. cosmogenic effects. Earth Planet. Sci. Lett. 242, 2–25.
Markowski, A., Leya, I., Quitté, G., Ammon, K., Halliday, A.N., Wieler, R., 2006b. Correlated helium-3 and tungsten isotopes in iron meteorites: quantitative cosmogenic corrections and planetesimal formation times. Earth Planet. Sci. Lett. 250, 104–115.
McKeegan, K.D., Davies, A.M., 2004. Early Solar System chronology. Treatise Geochem. 1, 431–460.
Mostefaoui, S., Lugmair, G.W., Hoppe, P., El Goresy, A., 2004. Evidence for live ^{60}Fe in meteorites. New Astron. Rev. 48, 155–159.
Mostefaoui, S., Lugmair, G.W., Hoppe, P., 2005. ^{60}Fe: a heat source for planetary differentiation from a nearby supernova explosion. Astrophys. J. 625, 271–277.
Moynier, F., Blichert-Toft, J., Telouk, P., Luck, J.-M., Albarède, F., 2007. Comparative stable isotope geochemistry of Ni, Cu, Zn and Fe in chondrites and iron meteorites. Geochim. Cosmochim. Acta 71, 4365–4379.
Niemeyer, S., 1985. Systematics of Ti isotopes in carbonaceous chondrite whole-rock samples. Geophys. Res. Lett. 12, 733–736.
Podosek, F.A., Ott, U., Brannon, J.C., Neal, C.R., Bernatowicz, T.J., Swan, P., Mahan, S.E., 1997. Thoroughly anomalous chromium in Orgueil. Meteorit. Planet. Sci. 32, 617–627.
Quitté, G., Meier, M., Latkoczy, C., Halliday, A.N., Günther, D., 2006a. Nickel isotopes in iron meteorites — nucleosynthetic anomalies in sulphides with no effects in metals and no trace of ^{60}Fe. Earth Planet. Sci. Lett. 242, 16–25.
Quitté, G., Zanda, B., Halliday, A.N., Latkoczy, C., Günther, D., 2006b. Search for ^{60}Fe in chondrules from Allende and Tieschitz. Lunar Planet. Sci. XXXVII abstract 1856.
Quitté, G., Halliday, A.N., Meyer, B.S., Markowski, A., Latkoczy, C., Günther, D., 2007. Correlated iron-60, nickel-62 and zirconium-96 in refractory inclusions and the origin of the Solar System. Astrophys. J. 655, 678–684.
Ranen, M.C., Jacobsen, S.B., 2006. Barium isotopes in chondritic meteorites: implications for planetary reservoir models. Science 314, 809–812.
Rotaru, M., Birck, J.-L., Allègre, C.J., 1992. Clues to early Solar System history from chromium isotopes in carbonaceous chondrites. Nature 358, 465–470.
Scherstén, A., Elliott, T., Hawkesworth, C., Russell, S., Masarik, J., 2006. Hf–W evidence for rapid differentiation of iron meteorite parent bodies. Earth Planet. Sci. Lett. 241, 530–542.
Scott, E.R.D., 1977. Composition, mineralogy and origin of Group IC iron meteorites. Earth Planet. Sci. Lett. 37, 273–284.
Shukolyukov, A., Lugmair, G.W., 1993a. Live iron-60 in the early Solar System. Science 259, 1138–1142.
Shukolyukov, A., Lugmair, G.W., 1993b. ^{60}Fe in eucrites. Earth Planet. Sci. Lett. 119, 159–166.
Shukolyukov, A., Lugmair, G.W., 2006. Manganese–chromium isotope systematics of carbonaceous chondrites. Earth Planet. Sci. Lett. 250, 200–213.
Tachibana, S., Huss, G.R., 2003. The initial abundance of ^{60}Fe in the Solar System. Astrophys. J. 588, L41–L44.
Tachibana, S., Huss, G.R., Kita, N.T., Shimoda, G., Morishita, Y., 2006. ^{60}Fe in chondrites: debris from a nearby supernova in the early Solar System? Astrophys. J. 639, L87–L90.

Takafuji, N., Hirose, K., Mitome, M., Bando, Y., 2005. Solubilities of O and Si in liquid iron in equilibrium with (Mg,Fe)SiO_3 perovskite and the light elements in the core. Geophys. Res. Lett. 32, L06313. doi:10.1029/2005GL022773.
Trinquier, A., Birck, J.-L., Allègre, C.J., 2007. Widespread ^{54}Cr heterogeneity within the inner Solar System. Astrophys. J. 655, 1179–1185.
Wade, J., Wood, B.J., 2005. Core formation and the oxidation state of the Earth. Earth Planet. Sci. Lett. 236, 78–95.
Wasserburg, G.J., Gallino, R., Busso, M., 1998. A test of the supernova trigger hypothesis with Fe-60 and Al-26. Astrophys. J. 500, L189–L193.
Yin, Q., Jacobsen, S.B., Yamashita, K., 2002. Diverse supernova sources of pre-solar material inferred from molybdenum isotopes in meteorites. Nature 415, 881–883.
Yokoyama, T., Rai, V.K., Alexander, C.M.O'D., Lewis, R.S., Carlson, R.W., Shirey, S.B., Thiemens, M.H., Walker, R.J., 2007. Osmium isotope evidence for uniform distribution of s- and r-process components in the early Solar System. Earth Planet. Sci. Lett. 259, 567–580.
Yurimoto, H., Kuramoto, K., 2004. Molecular cloud origin for the oxygen isotope heterogeneity in the Solar System. Science 305, 1763–1766.